Biochimica et Biophysica Acta, 1022 (1990) 215–228
Elsevier

BBAMEM 74724

Kinetic evidence that arachidonate-induced calcium efflux from platelet microsomes involves a carrier-type ionophoric mechanism *

Thomas H. Fischer, Anne M. Griffin **, David W. Barton and Gilbert C. White, II

Department of Medicine, Center for Thrombosis and Hemostasis and Dental Research Center, University of North Carolina at Chapel Hill, Chapel Hill, NC (U.S.A.)

(Received 15 June 1989)
(Revised manuscript received 10 October 1989)

Key words: Ionophore mechanism; Kinetics; Calcium ion transport; Platelet microsome; Arachidonic acid

Arachidonate, at concentrations up to 50 μM, induced dose-dependent calcium efflux from preloaded microsomes prepared from human platelets, but not from unilamellar egg phosphatidylcholine vesicles. Arachidonate-induced efflux from microsomes was not inhibited by indomethacin, 13-azaprostanoic acid, or catalase and superoxide dismutase, indicating that the release was due to arachidonate and not a metabolite. Linolenate (18:3, *cis*) and linoleate (18:2, *cis*) induced calcium efflux in a manner similar to arachidonate (20:4, *cis*), while arachidate (20:0), linolelaidate (18:2, *trans*), elaidate (18:1, *trans*), oleate (18:1, *cis*), stearate (18:0) and palmitate (16:0) had no effect. An experimental method was developed for distinguishing between carrier ionophore, small aqueous pore (i.e., calcium channel), or large aqueous pore (i.e., detergent effect) mechanisms in vesicular efflux systems in which calcium efflux occurs over a period of minutes. This development predicted that with a carrier ionophore mechanism, an increase in either internal or external calcium should competitively inhibit ^{45}Ca efflux. In contrast, ^{45}Ca efflux by diffusion through a small aqueous pore or a large aqueous pore should be measurably insensitive to variations in internal or external calcium. These predictions were experimentally verified in the platelet microsomal system using efflux agents with known mechanisms. Efflux of ^{45}Ca by A23187, a calcium ion carrier ionophore, was sensitive to internal or external calcium competition, while alamethicin, a small aqueous pore channel model, and Triton X-100, a detergent which forms large aqueous pores, mediated ^{45}Ca efflux which was measurably insensitive to variations in internal or external calcium concentration. Arachidonate-induced ^{45}Ca efflux was inhibited by increasing either internal and external calcium concentration, suggesting that the fatty acid functions as a carrier ionophore. Arachidonate-induced ^{45}Ca efflux was also inhibited with extravesicular Sr^{2+}, but not Mn^{2+} or Ba^{2+}. The dependence of the initial arachidonate efflux rate on arachidonate concentration showed that at least two arachidonates were contained in the calcium-carrier complex. These results are consistent with a model in which arachidonate (A) and an endogenous microsomal component (B) translocate calcium across the membrane through a carrier ionophore mechanism as part of a complex with a stoichiometry of $A_2B \cdot Ca$.

Introduction

Human platelets respond to agonists by a rapid increase in cytoplasmic levels of calcium followed by aggregation and secretion of granule contents [1]. The increase in cytoplasmic calcium as measured by intracellular calcium indicators such as Quin2, Fura-2, or aequeorin, correlates strongly with activation [2–4]. Although extracellular calcium appears to contribute in part to the rise in cytoplasmic calcium [4], the major source of calcium is believed to be intracellular storage sites such as the dense tubular system.

Studies of the mechanism by which calcium is re-

* The terms used in this paper are as defined by Läuger [42]. 'Carrier ionophore' refers to a transport system in which calcium dissociably complexes with a carrier molecule and is translocated across the membrane. 'Small aqueous pore' refers to an aqueous pore which is small enough for channel interaction within the primary hydration sphere of the ion. 'Large aqueous pore' refers to an aqueous pore which is large enough for an ion to diffuse through with an intact hydration sphere, without interaction with the pore.

** Present address: Department of Psychiatry, Cornell University Medical School, New York, NY, U.S.A.

Correspondence: T.H. Fischer, Center for Thrombosis and Hemostasis, University of North Carolina School of Medicine, Burnett-Womack Bldg 229H, Chapel Hill, NC 27599, U.S.A.

leased from subcellular storage sites have focused largely on products of membrane phospholipid metabolism. Gerrard and co-workers showed that prostaglandin (PG) endoperoxides, PGG_2 and PGH_2 but not PGD_2, PGE_1, or PGE_2, promote calcium release from a microsomal fraction derived from platelets [5]. They further showed that thromboxane A_2 bound calcium and transported calcium into diethyl ether [6]. Since thromboxane synthetase is a microsomal enzyme, it was suggested that thromboxane A_2 formed in the microenvironment of the dense tubular system initiated calcium release into the cell cytoplasm. Subsequent studies by these same workers [7] and by White and Raynor showed that products of phospholipase C metabolism, including phosphatidic acid, which is generated earlier in the phosphatidylinositol (PI) cycle, could also release calcium from microsomal stores [8]. More recently, studies by Berridge led to the hypothesis that inositol trisphosphate (IP_3) mediated the mobilization of intracellular calcium stores [9]. Using either permeabilized cells or calcium-loaded microsomal or intracellular membrane fractions, IP_3 has been shown to stimulate calcium release in platelets [10–13]. IP_3-mediated calcium release was inhibited by a monoclonal antibody to the microsomal membrane [14] suggesting that release was receptor mediated.

While the mechanisms described above are no doubt important for calcium changes during platelet activation by many agonists, other mechanisms appear to exist for some agonists and may provide alternate or amplification mechanisms for calcium mobiliation. For example, epinephrine has been shown to increase cytoplasmic calcium in platelets treated with aspirin [4], an agent which inhibits epinephrine-induced generation of prostaglandin endoperoxides, thromboxane A_2, and IP_3 [15]. Similarly, ADP, which does not induce hydrolysis of ^{32}P-labeled phosphatidylinositol 4,5-bisphosphate to IP_3 [16], increases cytoplasmic calcium in platelets treated with aspirin to inhibit generation of prostaglandin endoperoxides and thromboxane A_2 [17]. Although more recent data disputes IP_3 formation in ADP-stimulated platelets [18], these studies suggest that other phospholipid metabolites such as arachidonic acid may also play a role in calcium mobilization under certain conditions in platelets.

The studies presented here were undertaken to evaluate arachidonic acid as a calcium mobilizing agent in platelets. The results demonstrate that arachidonate is a potent calcium releasing agent and that the release of calcium is a specific effect that involves a carrier ionophore mechanism and is not due to detergent action of the lipid or activation of a calcium channel protein.

Materials and Methods

Materials. Egg phosphytidylcholine, octyl glucoside, hexokinase, adenosine triphosphate, Sephadex G-50, iminodiacetic acid agarose, catalase, superoxide dismutase, A23187, alamethicin, gramicidin D, and Triton X-100 were purchased from Sigma Chemical Corporation (St. Louis, MO). ScintiVerse-BD liquid scintillation fluid was from Fisher Scientific. Fatty acids were purchased as either the sodium salt or free acid from Sigma Chemical Corporation and were dissolved in ethanol as a stock solution of 20 mM and stored at $-20\,^\circ$C under N_2. Fatty acids included sodium arachidonate (20 : 4, *cis*), sodium linoleate (18 : 2, *cis*), linolenic acid (18 : 3, *cis*), arachidic acid (20 : 0), sodium oleate (18 : 1, *cis*), sodium stearate (18 : 0), sodium palmitate (16 : 0), linolelaidic acid (18 : 2, *trans*), and elaidic acid (18 : 1, *trans*). Arachidonate was further purified by reversed phase high pressure liquid chromatography (HPLC) using a 5 μm Ultrasphere ODS column (Altex Corp.). Fractions eluting as arachidonate were pooled, dried under N_2, and stored at $-80\,^\circ$C under N_2 until use which was within 5–7 days. Micropore filters (HAMK), 0.45 μm, were from the Millipore Corporation (Milford, MA). [^{45}Ca]Cl_2 (12.2 mCi/mg) and [^{3}H]arachidonate (90 mCi/mg) were obtained from ICN Biomedicals Inc. 13-Azaprostanoic acid was kindly provided by Dr. Guy LeBreton (Chicago, IL).

Platelet microsomes. The isolation of platelet microsomes was described in detail elsewhere [8]. Briefly, platelets were isolated from 200 ml of fresh blood from normal, healthy volunteer donors. The final platelet pellet was resuspended in one ml of 'sonication buffer' (94 mM KCl, 5 mM $MgCl_2$, 10 μM $CaCl_2$, 20 mM Tris/Tris-HCl (pH 7.0)) and sonicated in six 20-s bursts alternating with 20 s on ice. A $14000 \times g$ to $40000 \times g$ microsomal fraction was then isolated by differential centrifugation. The microsomes were loaded with calcium as previously described [19] by suspending the final microsomal pellet in 'incubation medium' (94 mM KCl, 5 mM $MgCl_2$, 50 μM $^{40}CaCl_2$, 0.5 μM $^{45}CaCl_2$, 2 mM ATP, 100 mM glucose, 5 mM KH_2PO_4/K_2HPO_4, 20 mM Tris/Tris-HCl (pH 7.0)) for 60 min at 21° C. Under these conditions, microsomes accumulate calcium in an ATP-dependent manner via a membrane associated Ca^{2+}-ATPase. Protein and phospholipid concentrations were measured by the method of Peterson [20] and Bartlett [21], respectively.

In experiments to determine the effect of internal calcium concentration on efflux, the microsomes were loaded with two different concentrations of calcium. For the preparation of microsomes containing high internal calcium, the 'incubation medium' defined above

(free total calcium = 25.4 μM) was used. For the preparation of microsomes with low internal calcium, and 'incubation medium' with 25 μM $^{40}CaCl_2$, 2.0 μM $^{45}CaCl_2$ and 50 μM EGTA (free total calcium = 0.45 μM) was used. After loading with calcium, $^{40}CaCl_2$ was added to microsomes with the low internal calcium sample to adjust the total external free calcium concentration in the two samples to the same value prior to the initiation of the efflux studies. The concentration of free calcium was calculated by the method of Fabiato and Fabiato [22].

Phospholipid vesicles. Calcium-loaded, unilamellar egg phosphatidylcholine (PC) vesicles were prepared by a chromatographic detergent depletion method [23]. Egg PC, 25 mg, was dried from $CHCl_3$ with N_2 and high vacuum, then solubilized with one ml of 'incubation medium' containing 200 mM octyl glucoside, 50 μM arsenazo III, 1 mM $^{40}CaCl_2$ and 1 μM $^{45}CaCl_2$. Vesicles were then formed by chromatography on a 1.2 × 30 cm column of Sephadex G-50 at a flow rate of 12 ml/h. The column was equilibrated and eluted with the same 'incubation medium' used for solubilization without detergent. The turbid fractions were pooled and applied to a second column of Sephadex G-50 of similar size which was equilibrated with the same 'incubation medium' that contained 50 μM $^{40}CaCl_2$ but no radioisotope or arsenazo III. Extravesicular medium exchange was then accomplished by elution at the same flow rate as the first column. The turbid fractions were pooled and immediately utilized for calcium transport studies. Negative staining electron microscopic [24] examination of the vesicles showed that they were unilamellar and had an average diameter of 200 nm. The entrapment of 1 mM $CaCl_2$ was verified by measuring the absolute amount of vesicular $^{45}CaCl_2$ with liquid scintillation counting and measuring the absorbance of the entrapped arsenazo III (at an internal concentration of 50 μM) to obtain the total internal volume.

Calcium efflux measurement. For measurement of calcium efflux from platelet microsomes, the microsomes, previously loaded with calcium, were treated with hexokinase to inhibit Ca^{2+}-ATPase activity and divided into equal volumes, depending on the number of samples required. Experiments were carried out at 21° C. Efflux was initiated by the addition of the test agent, fatty acid, ionophore, or detergent to the microsomes at a 1:100 dilution. At various time intervals after the addition of the agent, 100 μl portions were removed and rapidly filtered through 0.45 μm nitrocellulose filters. The filters were washed twice with 5 ml of iced saline, then placed in 5 ml ScintiVerse-BD for liquid scintillation counting to quantify the calcium remaining associated with the microsomes.

For measurement of calcium efflux from phospholipid vesicles, the concentration of the vesicles was adjusted with 'incubation medium' (containing 50 μM $CaCl_2$) to a phospholipid concentration of approx. 300 μM. Efflux was initiated by diluting test agent, fatty acid, ionophore, detergent, or an equivalent volume of ethanol carrier, into the vesicles at a dilution of 1:100. At various time intervals after the addition of the test agent, 100 μl of the vesicle suspension were removed and gel filtered on 1.0 ml minicolumns of iminodiacetic acid agarose equilibrated with 'incubation medium' at a flow rate of 1 ml/min to remove extravesicular $^{45}Ca^{2+}$. The internal calcium was quantified by counting the first 3.0 ml of eluate.

Arachidonate metabolism by microsomes. To hexokinase-treated, calcium-loaded microsomes was added one-hundredth volume of arachidonate that contained [^{3}H]arachidonate for a specific activity of 0.04 Ci/mmol. At intervals after the addition of arachidonate, samples were removed for determination of calcium efflux as described above, for measurement of thromboxane B_2 using a radioimmunoassay kit (NEN-Dupont, Wilmington, DE), and for analysis of arachidonate metabolism by reversed-phase HPLC. HPLC samples were extracted with chloroform/methanol and chromatographed using a 5 μm Ultrosphere ODS column preceded by a precolumn filter (0.5 μm frit, Upchurch Scientific, Oak Harbor, WA). Elution was at a flow rate of 1.1 ml/min with a complex linear gradient developed using water/methanol (9:1, v/v), pH 5.05, in pump A and methanol in pump B. Initial conditions were 47% pump A with linear changes in the gradient at the following time points: 27 min, 40% pump A; 52 min, 27% pump A; 74 min, 0% pump A. Radioactivity associated with individual peaks was quantified using a Flow-One CR Radioactivity Detector (Radioanalytic Instrument Co., Tampa, FL). Metabolite peaks were identified based on retention time compared with externally applied standards.

Calculation of initial calcium efflux rates from platelet microsomes. Efflux of internal calcium ($[Ca_i]$) from hexokinase-treated microsomes in the absence of arachidonate was exponential. Plots of $\log([Ca_i])$ vs. time gave approximately straight lines, the slope of which gave the apparent efflux rate constant for control efflux (k_c). Thus,

$$-d[Ca_i]/dt = k_c[Ca_i] = J_c \quad (1)$$

In the presence of arachidonate, efflux was also exponential, but with a larger apparent rate constant, $k_a + k_c$.

$$-d[Ca_i]/dt = (k_a + k_c)[Ca_i] = J_a + J_c \quad (2)$$

The initial rate of arachidonate-induced efflux (J_a^0) was obtained by measuring the slope of logarithmic plots of the efflux data in the absence and presence of arachidonate to obtain k_c and $k_a + k_c$, respectively. Thus,

$$-k_a = k_c - (k_a + k_c) \quad (3)$$

and

$$J_a^0 = k_a[Ca_i]^0 \quad (4)$$

where $[Ca_i]^0$ is the internal calcium concentration at the time of arachidonate addition which was estimated by dividing the moles of internalized calcium (obtained from the micropore filter dpm count and specific radioactivity of the 'incubation medium') by the internal volume of the microsomes (assumed to be 2.85 μl/mg protein [25]) *. The initial efflux rate of calcium ($^{40}J_a^0$ and $^{45}J_a^0$) was calculated from the specific radioactivity of calcium in the 'incubation medium'.

Calculation of the stoichiometry of arachidonate activation. The procedure used to calculate the stoichiometry of arachidonate is similar to that of Meyer et al. [26] and assumes a translocation mechanism in which the steady-state approximation applies and the rate limiting step involves carrier-calcium ion movement across the membrane. The carrier complex is assumed to be of the form $A_\alpha(B_\beta^1 B_\gamma^2 B_\delta^3 \ldots)Ca$, where A refers to arachidonate, B^1, B^2, and B^3 refer to endogenous membrane components, and greek letters are stoichiometric subscripts. The complex is assumed to partially or completely disassemble with each turn of the translocation cycle, as has been described for A23187 and X537A [27,28]. Knowledge of the exact assembly-disassembly pathway is not necessary for the following development. The flux of calcium is proportional to the concentration of the complex that immediately precedes the rate-limiting step, which is a function of the total membrane-bound arachidonate concentration, $[A_t]$

$$J_a = k\left[A_\alpha(B_\beta^1 B_\gamma^2 B_\delta^3 \ldots)Ca_i\right]$$

$$= k[A]^\alpha[B^1]^\beta[B^2]^\gamma[B^3]^\delta \ldots [Ca_i]/K_{app} \quad (5)$$

where k is the first-order rate constant for the translocation step and K_{app} is an apparent dissociation constant for the equilibria leading to complex formation.

$$K_{app} = \frac{[A]^\alpha[B^1]^\beta[B^2]^\gamma[B^3]^\delta \ldots [Ca_i]}{[A^\alpha(B_\beta^1 B_\gamma^2 B_\delta^3 \ldots)Ca_i]} \quad (6)$$

A logarithmic derivative of Eqn. 6 can be used to establish a lower limit of the value of α in terms of the known quantities $[A_t]$ (calculated by the method of Tanford [29] as the positive root of $([A_{add}] - [A_t])([A_t] + [PL]) = [A_t][A_{cmc}]$, where $[A_{add}]$ is the concentration of total added fatty acid, [PL] is the microsomal phospholipid concentration [21], $[A_{cmc}]$ is the critical micelle concentration of arachidonate (7 μM, the point at which turbidity was optically measured with arachidonate in our buffer system) and J_a (obtained from the efflux measurements).

$$\frac{d(\log J_a)}{d(\log[A_t])} = \alpha\frac{d(\log[A])}{d(\log[A_t])} + \beta\frac{d(\log[B^1])}{d(\log[A_t])} + \ldots \frac{d(\log[Ca_i])}{d(\log[A_t])} \quad (7)$$

At low arachidonate concentrations, where:

$$[A_t] \ll K_{app}/[B^1]^\beta[B^2]^\gamma[B^3]^\delta \ldots [Ca_i] \quad (8)$$

equilibria leading to complex formation favor the free fatty acid, and thus $[A] \cong [A_t]$. Also, at low $[A_t]$, the concentrations of the other free components in the transporting complex are approximately equal to the total quantities, and undergo only small relative changes as $[A_t]$ is varied. Thus, in the limit of $[A_t] \to 0$, the derivative in Eqn. 7 gives the arachidonate stoichiometry:

$$\lim_{[A_t]\to 0} \frac{d(\log J_a)}{d(\log[A_t])} = \alpha \quad (9)$$

In the presence of high levels of added arachidonate, equilibria leading to complex formation are saturated and the addition of more fatty acid results in little transporting complex formation. With these conditions, J_a assumes a constant value and the derivative in Eqn. 7 approaches zero. As arachidonate concentration is varied from zero to saturating values, the derivative in Eqn. 7 varies continuously from a maximum value of α to zero. This is because the derivatives involving components other than arachidonate in Eqn. 7 assume negative values as the concentration of these free components decreases with increased $[A_t]$, e.g. as free components are incorporated into the transporting complex. The slope of log (J_a) versus $[A_t]$ thus gives a lower limit on the value of α.

Results

Upon exposure to ATP and calcium, platelet microsomes actively accumulate calcium through the activity of a Ca^{2+}-ATPase. Removal of ATP by the addition of hexokinase terminates active transport and the subsequent passive efflux of calcium follows a slow, exponential time-course (solid circles, Fig. 1A). The addition of arachidonate results in a concentration-dependent increase in calcium efflux with half-maximal efflux at 65 min at approx. 20 μM arachidonate (Fig. 1A). Fig. 1B shows a plot of log($[Ca_i]$) vs. time which was used to calculate J_a^0 for each arachidonate concentration. At 30 μM arachidonate, there was an approximately 5-fold acceleration in the initial rate of calcium efflux, from a

* The internal volume of microsomal vesicles arrived at by Le Peuch and co-workers is an estimate of the volume for all the microsomal vesicles. However, only a fraction of the microsomal vesicles are in the proper orientation for transport and retain calcium.

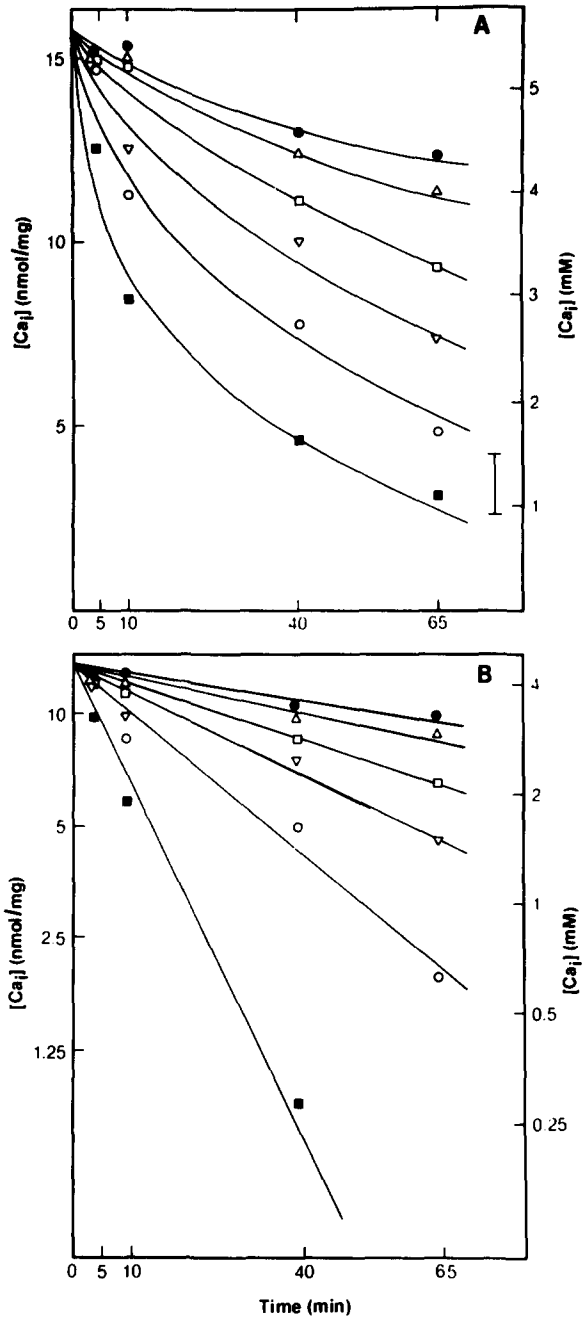

Fig. 1. The effect of arachidonate on calcium efflux from microsomes. Platelet microsomes were actively loaded with calcium as described in Materials and Methods. Uptake was then terminated and arachidonate or an equivalent amount of ethanol carrier was diluted 1/100 into the reaction mixture at time zero for [arachidonate] = 0 μM (●), 5 μM (△), 10 μM (□), 20 μM (▽), 30 μM (○), or 50 μM (■). Internal calcium was quantified with the micropore filtration assay. (Panel A) Plot of internal calcium as nmol/mg protein or concentration versus time. The error bar in the lower right hand corner of the panel shows the mean and standard deviation of the internal calcium remaining after the microsomes were treated with A23187. (Panel B) Plot of log[internal calcium] versus time. For this graph, the internal calcium remaining after A23187 was subtracted from each efflux value.

value of $1.2 \cdot 10^{-5}$ (J_c^0) to $6.5 \cdot 10^{-5}$ ($J_a^0 + J_c^0$) mol/liter per min. Similar results were obtained whether the free fatty acid or sodium salt were used.

To determine if the effect of Fig. 1 was due to the arachidonate or an arachidonate metabolite generated during efflux, a series of experiments were performed to either prevent metabolism of arachidonic acid or block the effect of arachidonic acid metabolites. To see if arachidonic acid was being metabolized to other products, the experiment in Fig. 1 was performed using 30 μM arachidonate containing a trace amount of [^{3}H]arachidonate. Samples were removed at the same intervals for calcium efflux and for analysis of the radioactive arachidonate metabolites by HPLC. Less than one percent of the recovered arachidonate was metabolized, primarily to thromboxane B_2 and 12-hydroxy-5,8,10-heptadecatrienoic acid (HHT). Levels of thromboxane B_2 measured by radioimmunoassay before and 40 min after addition of arachidonic acid were 0.37 ± 0.21 and 2.5 ± 0.35 ng/mg (mean ± S.D. of three experiments). The addition of 100 μM indomethacin to the microsomes 10 min prior to the addition of arachidonate had no effect on arachidonate-induced efflux, but completely inhibited the metabolism of arachidonate as measured by HPLC. Levels of thromboxane B_2 measured by radioimmunoassay before and 40 min after addition of arachidonic acid in the indomethacin-treated microsomes were 0.31 ± 0.17 and 1.94 ± 0.30 ng/mg. In similar experiments, the addition of 20 μM 13-azaprostanoic acid, a thromboxane and prostaglandin endoperoxide antagonist, had no effect on arachidonic acid-induced release of calcium. The addition of catalase and superoxide dismutase to final concentrations of 100 units/ml 10 min prior to treatment with arachidonate also had no effect on arachidonate-mediated efflux. Finally, the addition of thromboxane/prostaglandin endoperoxide analogs, U44619 and U46609, at concentrations up to 50 μM did not induce calcium release from preloaded platelet microsomes.

The ability of other fatty acids to release calcium from platelet microsomes is shown in Fig. 2. Linoleate (18 : 2, *cis*) and linolenate (18 : 3, *cis*) induced efflux of calcium similar to arachidonate (20 : 4, *cis*) while arachidate (20 : 0) and oleate (18 : 1, *cis*) did not release calcium. Stearate (18 : 0), palmitate (16 : 0), linolelaidic acid (18 : 2, *trans*), and elaidate (18 : 1, *trans*) were also tested and did not release calcium (data not shown).

Since the concentrations of arachidonate that induced calcium release were above the critical micelle concentration for arachidonate in the buffer system used, the effect of arachidonate on small unilamellar egg phosphatidylcholine vesicles that contained calcium was investigated to assess the possibility that the arachidonate-induced release was a detergent effect. The results are presented in Fig. 3. Arachidonate, in concentrations up to 50 μM, did not release calcium from the vesicles. Calcium was completely released by 2 μM ionophore A23187 or by 50 μM Triton X-100, indicat-

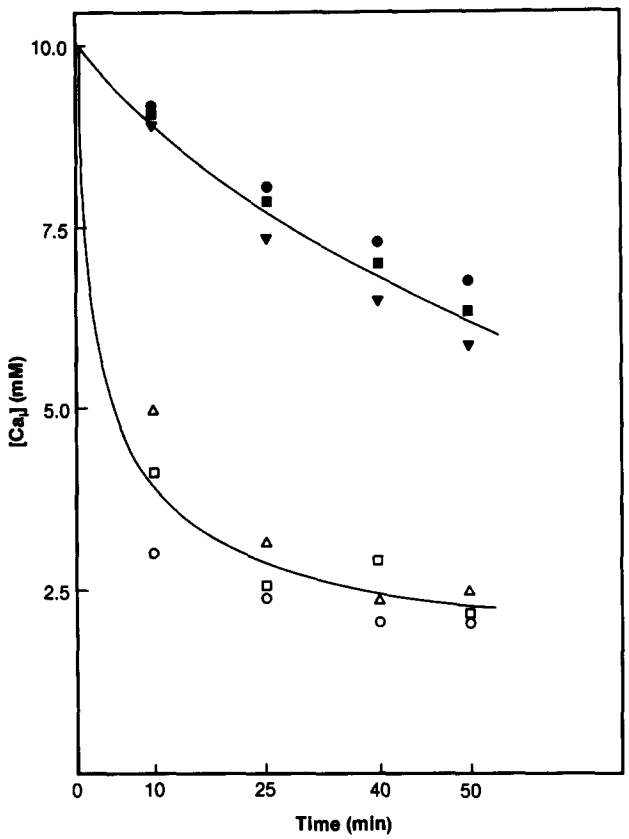

Fig. 2. Structural specificity of long chain fatty acids for induced calcium release. Microsomes were actively loaded with calcium and the uptake process terminated as in Fig. 1. At 0 min, 100/1 dilutions of ethanol (●) or ethanolic stock solutions of arachidonate (20:4, *cis*) (○); linoleate (18:2, *cis*) (□); linolenate (18:3, *cis*) (△); arachidate (20:0) (▼) and oleate (18:1, *cis*) (■) were added for amphiphile concentrations of 50 μM.

ing that the entrapped calcium was in a form that could be released.

As presented in Appendix A, a carrier ionophore

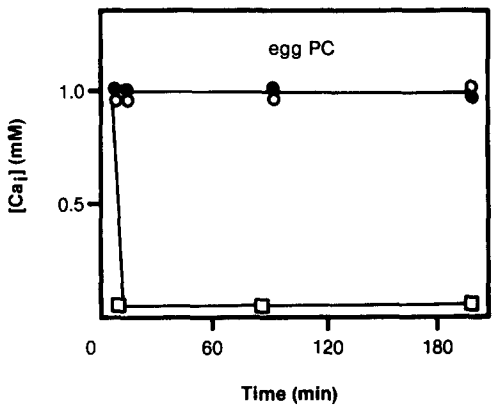

Fig. 3. Effect of arachidonate on calcium efflux from liposomes. Egg phosphatidylcholine unilamellar vesicles were formed in the presence of 1 mM calcium as outlined in Materials and Methods. At time zero, arachidonate, A23187 or ethanol carrier was diluted 1/100 for [arachidonate] = 50 μM (○), [A23187] = 20 μM (□) and zero efflux agent (●). Internal calcium was measured with the chelation chromatography method.

mechanism in a vesicle system is sensitive to variations in divalent ion levels; while transport through small aqueous pores* and large aqueous pores are insensitive to changes in calcium concentration under the conditions used in these experiments. To examine further the mechanism of calcium release by arachidonate, competitive inhibition of arachidonate-induced efflux of intravesicular ^{45}Ca by extravesicular $CaCl_2$ was studied. The addition of 10 mM $CaCl_2$ to the extravesicular medium completely inhibited the effect of arachidonate, and did not effect the control rate of efflux obtained when ethanol carrier was added to the reaction mixture (Fig. 4A). Complete inhibition of arachidonate-induced efflux was also obtained when the extravesicular calcium concentration was elevated to 10 mM at times up to 90 min after the addition of arachidonate, after substantial amounts of ^{45}Ca had effluxed through the arachidonate mechanism (data not shown). The addition of 10 mM extravesicular $SrCl_2$ gave the same result as $CaCl_2$ (data not shown), completely inhibiting fatty acid induced efflux, while 10 mM $BaCl_2$ or $MnCl_2$ did not affect arachidonate-induced efflux or control efflux. At a final concentration of 1 μM, gramicidin D did not affect arachidonate (30 μM) or A23187 (30 nM) mediated calcium efflux (data not shown) indicating that proton ion or other monovalent ions did not play a limiting role in the efflux mechanism of arachidonate or A23187.

Efflux experiments are presented in Figs. 4B, 4C and 4D with A23187, alamethicin and Triton X-100 as controls for carrier ionophore, small aqueous pore, and large aqueous pore, respectively. The addition of 10 mM $CaCl_2$ to the extravesicular space inhibited A23187-induced ^{45}Ca efflux, but had no effect on calcium release by alamethicin or Triton X-100. These efflux mechanism controls thus behaved as predicted by the kinetic development in the Appendix.

The dose dependence of the inhibitory effect of extravesicular $CaCl_2$ on arachidonate- and A23187-induced ^{45}Ca efflux is depicted in Fig. 5. Both arachidonate- and A23187-induced efflux were similarly inhibited by extravesicular calcium, with half-maximal inhibition obtained at approx. 2 mM $CaCl_2$. The shape of the inhibition curve closely matched the shape of the theoretically derived inhibition curve for a carrier mechanism presented in Appendix Fig. A-2.

To test for competition between intravesicular ^{40}Ca and ^{45}Ca for the arachidonate efflux mechanism, two samples of microsomes were prepared with similar concentrations of internal ^{45}Ca but differing concentrations of internal ^{40}Ca as detailed in Materials and Methods. The initial rates of internal ^{45}Ca and ^{40}Ca efflux in

* See footnote on p. 215.

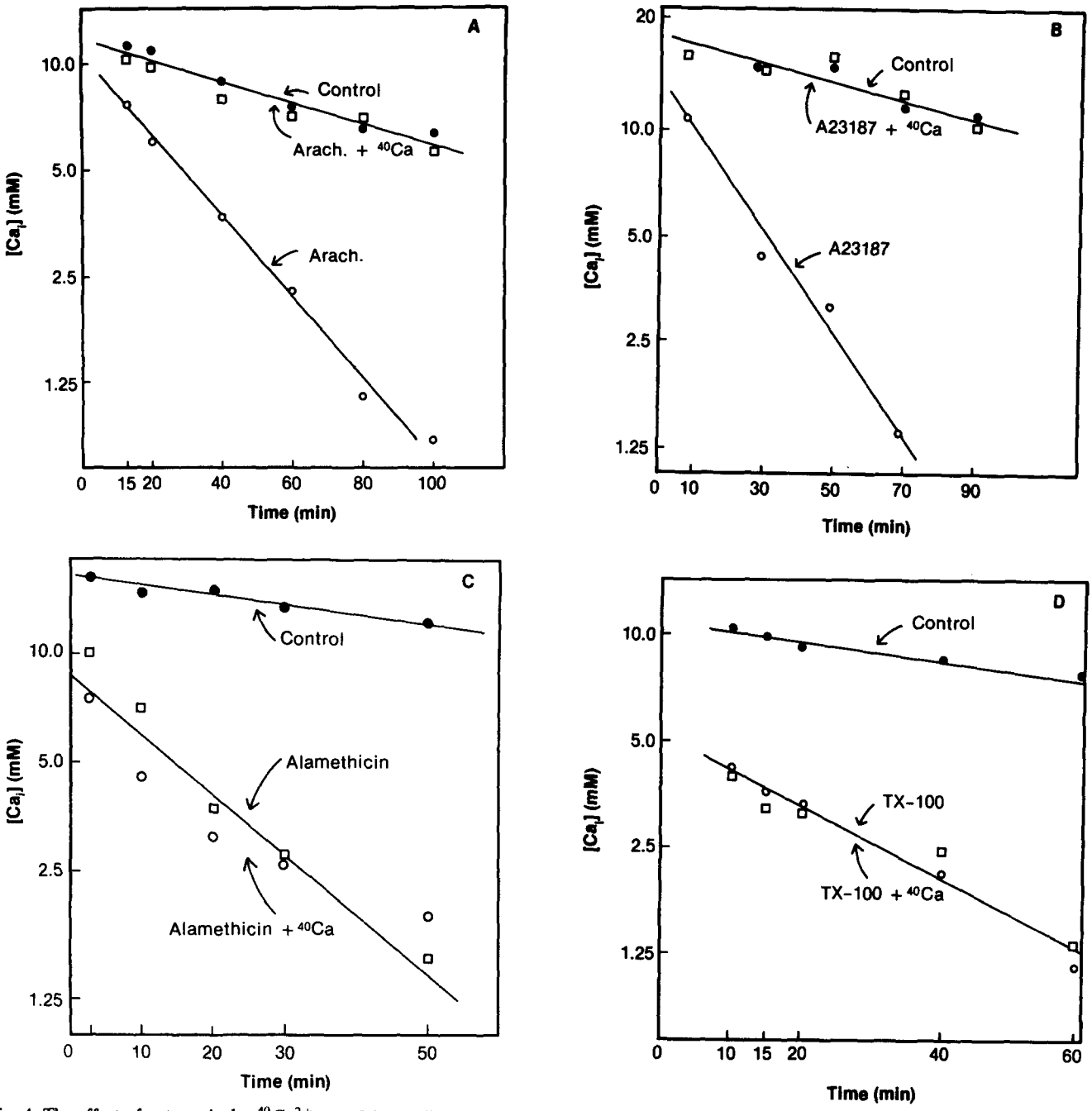

Fig. 4. The effect of extravesicular $^{40}Ca^{2+}$ on calcium efflux mechanisms. Microsomes were actively loaded with calcium as described in Fig. 1. (Panel A) At 0 min, arachidonate or ethanol was diluted 1/100 into the reaction mixtures for arachidonate concentrations of 30 μM or zero. At 2 min, $^{40}CaCl_2$ or H_2O was diluted 1/100 into the samples for final [$^{40}Ca_o$] of 10 mM or 0.05 mM. Arachidonate + H_2O (○), arachidonate + ^{40}Ca (□), ethanol + ^{40}Ca (●). (Panel B) At 0 min, A23178 or DMSO was diluted 1/100 into the reaction mixtures for A23187 concentrations of 30 nM or zero. At 2 min, $^{40}CaCl_2$ or H_2O was diluted 1/100 into the samples for final [^{40}Ca] of 10 mM or 0.05 mM. A23187 + H_2O (○), A23187 + ^{40}Ca (□), DMSO + ^{40}Ca (●). (Panel C) At 0 min, alamethicin or DMSO was diluted 1/100 into the reaction mixtures for alamethicin concentrations of 100 nM or zero. At 0.5 min, $^{40}CaCl_2$ or H_2O was diluted 1/100 for final [^{40}Ca] of 5 mM or 0.05 mM. Alamethicin + H_2O (○), alamethicin + ^{40}Ca (□), DMSO + ^{40}Ca (●). (Panel D). At 0 min, Triton X-100 or H_2O diluted 1/100 into the reaction mixtures for Triton X-100 concentrations of 100 μM or zero. At 2 min, $^{40}CaCl_2$ or H_2O was diluted 1/100 into the samples for final [^{40}Ca] of 10 mM or 0.05 mM. Triton X-100 + H_2O (○), Triton X-100 + ^{40}Ca (□), H_2O + ^{40}Ca (●).

response to 20 μM arachidonate were then measured and are presented in Table I. The results show that the internal ^{40}Ca competed for the efflux mechanism, while activating total arachidonate mediated ($^{40}J_a^0 + {}^{45}J_a^0$) efflux. An 8-fold increase in internal ^{40}Ca reduced the efflux rate of ^{45}Ca by approximately 60%, while stimulating total efflux of calcium 2.6-fold.

The definition of a carrier ionophore mechanism for arachidonate by the calcium isotope competition experiments was used in conjunction with the dose-depen-

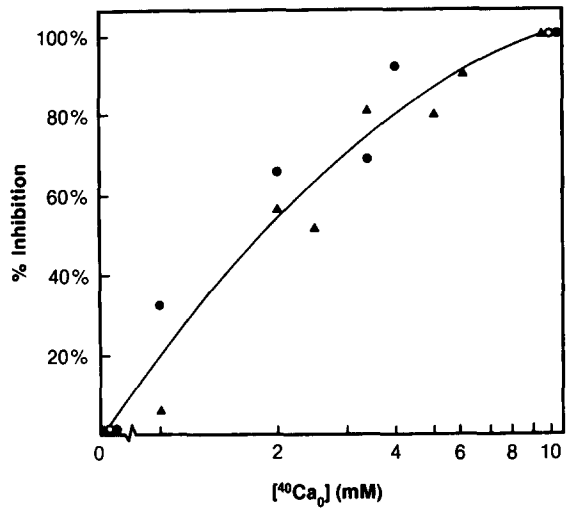

Fig. 5. Dose dependence of extravesicular calcium inhibition. $^{40}CaCl_2$ concentration on percent inhibition of the initial efflux rate induced by 30 μM arachidonate (●) and 30 nM A23187 (▲). Experimental details were as in Fig. 4.

dence data presented in this section to ascertain a lower limit for the number of arachidonates in the transporting complex. The dependence of initial efflux rate on the arachidonate concentration is depicted in Fig. 6. The fatty acid induced calcium efflux increased in a non-saturatable manner with the amount of added arachidonate, with measurable arachidonate-induced efflux rates being obtained above concentrations of 5 μM, and becoming too fast to measure with the micropore filtration method at concentrations above 50 μM. At all tested concentrations, efflux was exponential. The $\log(J_a^0)$ vs. log(mole fraction bound arachidonate) plot in Fig. 6 gives a straight line with a slope of 1.43. With the analysis method outlined in Materials and Methods,

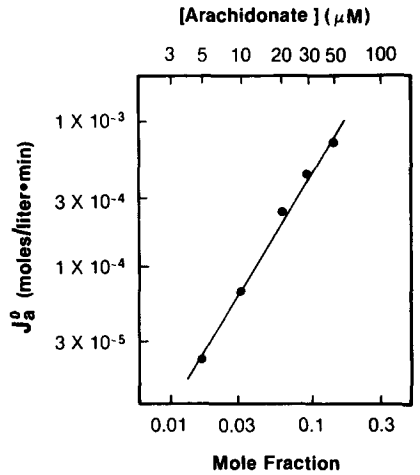

Fig. 6. The concentration dependence of the arachidonate-induced calcium efflux rate. Microsomes were actively loaded with calcium with Ca^{2+}-ATPase termination as in Fig. 1. At 0 min, the reaction mixture was proportioned and arachidonate or ethanol carrier diluted 1 : 100 into the samples. J_a^o was measured as detailed in Materials and Methods.

TABLE I

Competition of internal calcium isotopes for efflux

$[^{45}Ca_i]$ (mol/l)	$[^{40}Ca_i]$ (mol/l)	$^{45}J_a^o$ (mol/l per min)	$^{40}J_a^o$ (mol/l per min)	$^{40}J_a^o + ^{45}J_a^o$ (mol/l per min)
$1.5 \cdot 10^{-4}$	$1.5 \cdot 10^{-2}$	$3.34 \cdot 10^{-7}$	$3.27 \cdot 10^{-5}$	$3.30 \cdot 10^{-5}$
$1.4 \cdot 10^{-4}$	$1.8 \cdot 10^{-3}$	$8.8 \cdot 10^{-7}$	$1.21 \cdot 10^{-5}$	$1.30 \cdot 10^{-5}$

this value establishes a lower limit of two arachidonates in each calcium transporting complex.

Discussion

Although calcium appears to be a second messenger in most mammalian cells, the mechanisms of calcium release remain unclear in many instances. Numerous potential mechanisms have been described, including plasma and subcellular membrane calcium channels, plasma membrane calcium exchangers, and submembranous calcisomes. In platelets, which have active lipid metabolic systems, products of phospholipid metabolism have been implicated in the release of calcium from subcellular stores during cell activation. Prostaglandin endoperoxides, thromboxanes, phosphatidic acid, and inositol trisphosphate have been shown to release calcium from platelet microsomal fractions in vitro. The results of the present study indicate that arachidonic acid is also able to release calcium from platelet microsomes.

Previous studies by Gerrard and co-workers have shown that arachidonic acid was able to release calcium from platelet microsomes and that pretreatment of intact platelets with aspirin prior to preparation of microsomes inhibited the arachidonic acid induced release [5]. However, the amount of calcium released was very small. Subsequent studies by Rybicki et al. confirmed the effect of arachidonate and showed that the release of calcium by arachidonate was blocked by 13-azaprostanoic acid, a thromboxane and prostaglandin endoperoxide antagonist, indicating that the arachidonic acid-induced release was mediated by prostaglandin endoperoxides and/or thromboxane A_2 generated from arachidonic acid [30]. The results presented here indicate that under certain conditions, arachidonate itself is able to release calcium and is able to release larger amounts of calcium that other putative calcium release agents such as inositol trisphosphate [11–13]. The reason for the difference between our results and those of Gerrard and co-workers and Rybicki and co-workers is not readily apparent. The preparation of microsomes in our study and that of Rybicki is essentially similar except that in the present study, the microsomes were prepared freshly. For calcium uptake, we have used a non-precipitating counterion, phosphate, which has allowed accumulation of larger amounts of calcium. This

may have increased the sensitivity of our system to an arachidonic acid effect compared with that of Rybicki and co-workers, who did not use a counterion. Finally, basal levels of thromboxane B_2 in the freshly prepared microsomes used in these studies were 10-fold lower than in those used by Rybicki and co-workers. The higher basal thromboxane levels in the membranes prepared by Rybicki suggests that their membranes may have had, for some reason, an intact arachidonate metabolizing system which could have precluded observation of an arachidonate effect.

The evidence that it is arachidonate that mediates efflux and not a metabolite, an oxidative product, or a contaminant of arachidonate, derives from four studies. First, inhibition of arachidonic acid metabolism by indomethacin, which was confirmed by HPLC and radioimmunoassay for thromboxane B_2, did not inhibit the arachidonic acid effect. Second, 13-azaprostanoic acid, which is a thromboxane A_2 and prostaglandin endoperoxide antagonist, did not inhibit the arachidonic acid effect. Third, thromboxane A_2 and prostaglandin endoperoxide analogs, U44619 and U46609, were not able to release calcium from preloaded microsomes. Fourth, the addition of catalase and superoxide dismutase, which scavenge oxygen radicals [31], did not affect arachidonate-mediated efflux.

Does arachidonate mediated efflux require an endogenous cofactor?

The results presented in Fig. 3 and the reports of others [32] that arachidonate does not release calcium from model membrane vesicles suggests that arachidonate requires one or more endogenous membranes components to function as a calcium transporter. The implication of this finding is that in the absence of the membrane component, arachidonate is either unable or incompetent to form a transporting mechanism. It is not clear from these studies what the endogenous component is or how it interacts with arachidonate.

Does arachidonate induced efflux involve a carrier, channel, or bilayer defect?

Studies with A23187 and other calcium carrier ionophores have shown that carrier-mediated transport mechanisms are rate limited by relatively slow translocation step(s) which occur with each turn of the transport cycle and that other steps involving carrier complex formation are in approximate equilibrium [27,28]. As a consequence, the efflux rate would be expected to be sensitive to variations in calcium concentration through linked equilibria. An increase in internal ^{40}Ca should reduce the amount of internal carrier that is complexed with ^{45}Ca and will therefore reduce the efflux rate of ^{45}Ca even though total Ca efflux may increase. In a similar manner, an increase in external ^{40}Ca (or other divalent cations that can form a complex with external facing carrier) should shift equilibrium away from the internal carrier-radioisotope complex, yielding a net reduction in ^{45}Ca efflux. These were indeed the results obtained with both A23187 and arachidonate. Thus, arachidonate appears to transport calcium by a carrier ionophore mechanism. The ability of extravesicular strontium, but not barium or manganese, to inhibit arachidonate mediated ^{45}Ca efflux indicates that bivalent cations other than calcium can shift equilibrium away from the transporting complex, and is evidence for selectivity of the arachidonate mechanism.

In contrast, efflux through large aqueous pores, such as those created by detergents, or through small aqueous pores are extremely rapid. Kinetic studies of a variety of calcium channels [33–39] and model small aqueous pores, such as gramicidins [40] and alamethicin [38], indicate that once a channel is open, transport through the pore occurs rapidly enough to discharge the calcium content of the vesicle within milliseconds or less. Competition between ^{40}Ca and ^{45}Ca in such a system would take place only during the few milliseconds that the individual vesicle is discharging the divalent ion gradient. However, in a system where efflux of calcium is measured over minutes, the internal calcium at any given point in time represents an average value from three populations of vesicles: vesicles that have not had an open channel and contain the initial calcium concentration, vesicles that have had an open channel and discharged the calcium gradient, and vesicles that have an open channel and are in the process of effluxing the calcium gradient. Only the discharging vesicles are kinetically sensitive to variations in divalent ion concentration, but since the discharge process takes place over a period of several milliseconds, discharging vesicles represent a minuscule fraction of the total vesicle population. Thus, while the kinetic properties of calcium channels are sensitive to divalent cation when examined on a single-channel basis, micropore filtration assays performed over a period of minutes would not be measurably sensitive to variations in calcium concentrations. Similar stochastic kinetics hold for free diffusion through a large aqueous pore, except that even the small population of vesicles that are effluxing the calcium would be insensitive to variations in divalent cation concentrations because of the weak concentration dependence of the calcium diffusion coefficient [41]. Thus, our results with arachidonate are not kinetically consistent with efflux involving an arachidonate-gated small aqueous pore or large aqueous pore.

The simplest (and entropically most favorable) model that is consistent with the presented data is that arachidonate forms a carrier complex that contains a calcium, two arachidonate molecules, and an endogenous membrane component (B). The involvement of at least two arachidonates in the calcium translocation process is

based on the slope of the activation curve in Fig. 6. The measurement of a value of 1.43 for the slope in Fig. 6 means that two or more arachidonates are required to form the transporting complex (see Materials and Methods for details of the calculation). While the reported experiments establish a lower limit on the complexity of the transporting complex ($A_2B \cdot Ca$), the coordination number of six to eight for the divalent calcium ion places an upper constraint on the number of components that can interact with the ion as part of a carrier complex. Thus, if the complex contains two arachidonate molecules, a maximum of six endogenous components would be able to interact with the ion. However, the entropic cost of having a transporting complex that contains a larger number of separate components favors the possibility that there is a minimum number of endogenous species. Based on analogy with A23187 (and similar carrier ionophores, such as X537A), it is proposed that the transporting complex is stabilized by the calcium ion; the unligated A23187 dimer plays an insignificant role in the transport cycle [27,28]. The preferred pathway of complex assembly likely involves binding of the cation to B, since the affinity of calcium for the single carboxyl group on the arachidonate molecule is low. After the calcium ion is confined to the interface of the membrane by the endogenous component, the second order reactions involving the addition of arachidonates to the complex would be accelerated since the components are effectively concentrated in the two-dimensional plane of the membrane. The requirement of the arachidonate carrier complex for at least four components (two arachidonates, a calcium ion and the endogenous component), while the A23187 complex contains only three components (two A23187 monomers and the calcium ion), might account for the 1000-fold difference in A23187 and arachidonate concentrations required to obtain a similar calcium efflux rate, the additional arachidonate being required to overcome the entropic cost of a complex containing an extra membrane component.

In summary, evidence that arachidonic acid can mobilize calcium from subcellular stores in platelets has been presented. This is a direct action of arachidonic acid and is inhibited by increasing the concentration of external calcium. Kinetic data for arachidonate-induced efflux of calcium are consistent with a carrier ionophore mechanism.

Appendix

The sensitivity of efflux mechanisms to variations in intra- and extravesicular calcium

The following analysis details how three types of efflux mechanisms are effected by changes in intra- and extravesicular calcium levels, and if such effects are detectable in a vesicular system when the measured calcium gradients are discharged over a period of minutes. The principle result is that carrier ionophore mechanisms with a rate-limiting slow step in each translocation cycle can be modulated by changes in the divalent ion concentration, while small aqueous pore mechanisms, which are rate limited by activation steps that are branched from the transport cycle, and large aqueous pore mechanisms, which are diffusion limited, are measurably insensitive to calcium concentration. The following sections provide the kinetic basis for this distinction.

(A) Carrier ionophores: mechanisms that are rate limited in the transport cycle

This type of mechanism is exemplified by carrier ionophores such as A23187, which functions as detailed in Fig. A-1. Studies in model vesicle systems have demonstrated that the rate-limiting step with carrier ionophores usually involves the translocation of the calcium ion across the membrane, and that the other reactions in the translocation cycle are in approximate equilibrium [27,28]. Under these conditions, the efflux rate is given by the following rate expression where k is the rate constant for the translocation step.

$$-\mathrm{d}([^{45}Ca_i])/\mathrm{d}t = k[A \cdot {}^{45}Ca_i] \qquad \text{(A-1)}$$

Steady-state methods [43] utilizing the equilibria involving the constants K_1 and K_2

$$K_1 = [A_i][{}^{45}Ca_i]/[A \cdot {}^{45}Ca_i] = [A_o][{}^{45}Ca_o]/[A \cdot {}^{45}Ca_o]$$
$$= [A_i][{}^{40}Ca_i]/[A \cdot {}^{40}Ca_i] = [A_o][{}^{40}Ca_o]/[A \cdot {}^{40}Ca_o]$$
$$K_2 = [A_i][A^{45}Ca_i]/[A_2 \cdot {}^{45}Ca_i] = [A_o][A^{45}Ca_o]/[A_2 \cdot {}^{45}Ca_o]$$
$$= [A_i][A^{40}Ca_i]/[A_2 \cdot {}^{40}Ca_i] = [A_o][A^{40}Ca_o]/[A_2 \cdot {}^{40}Ca_o] \qquad \text{(A-2)}$$

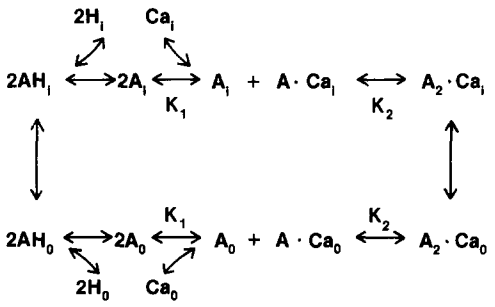

Fig. A-1. Transport scheme for A23187. Kinetic model for A23187 action proposed by Pfeiffer et al. (1978) and Kolber and Haynes (1981). Horizontal steps involve complex assembly on the inside and outside interfaces of the membrane. Vertical steps describe complex movement across the membrane. A, Ca, and H refer to A23187, ionized calcium, and hydrogen, respectively. The i and o subscripts on ions refer to the ions in the internal and external vesicular space, respectively. The i and o subscripts on the membrane-bound components for the other species in the diagrams refer to species oriented to the interior or exterior of the microsomes, respectively.

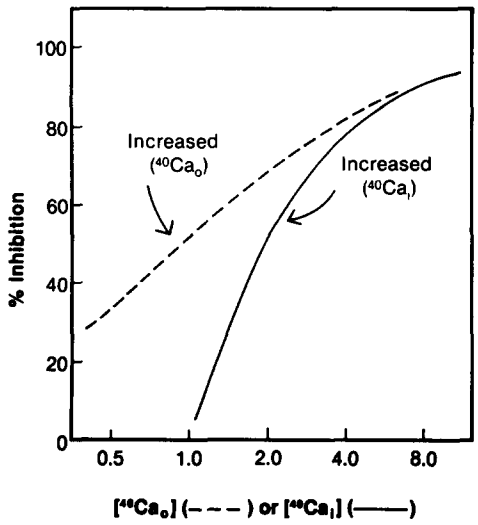

Fig. A-2. The response of a carrier to variations in internal calcium and external calcium. The curves are from Eqn. A-4 with $K_1 = 3 \cdot 10^{-3}$ M, $K_2 = 1 \cdot 10^{-3}$ M, $[^{45}Ca_i] = 1 \cdot 10^{-5}$ M, $[^{45}Ca_o] = 1 \cdot 10^{-8}$ M, $[A_t] = 1 \cdot 10^{-8}$ M, [phospholipid] $= 1 \cdot 10^{-4}$ M. Reference conditions with which percentage inhibition was compared: $[^{40}Ca_i] = 1 \cdot 10^{-3}$ M, $[^{40}Ca_o] = 1 \cdot 10^{-6}$ M. Internal calcium variation with fixed external calcium at reference value (———). External calcium variation at fixed internal calcium reference value (– – –).

and the mass conservation relationship for the ionophore, yield an expression for $[A^{45}Ca]$ and the efflux rate that depends only on internal and external ion concentrations. With the assumption that steps involving the protonation of free ionophore and the translocation of the protonated ionophore across the membrane can be simplified as:

$$A_i \underset{k_b}{\overset{k_f}{\rightleftharpoons}} A_o, \quad k_f = k_b \tag{A-3}$$

with an equilibrium constant of one, Eqn. A-1 becomes:

$$d([^{45}Ca_i])/dt = k\left[\left(b - (b^2 - 4ac)^{1/2}/2a\right]^2\right.$$

with

$$a = 2\left(1 + [^{45}Ca_o]/\left[^{45}Ca_i\right] + [^{40}Ca_i]/[^{45}Ca_i] + [^{40}Ca_o]/[^{45}Ca_i]\right)$$

$$b = \left(K_2[^{45}Ca_i]/K_1\right)^{1/2}(1 + [^{40}Ca_i]/[^{45}Ca_i]$$

$$+ \left(K_2[^{45}Ca_o]/K_1[^{45}Ca_i]\right)^{1/2}(1 + [^{40}Ca_o]/[^{45}Ca_o])$$

$$+ 2(K_1K_2/[^{45}Ca_i])^{1/2}$$

$$c = [A_t] \tag{A-4}$$

The behavior of Eqn. A-4 upon varying the internal and external $[^{45}Ca]$ is presented in Fig. A-2, which shows that transport of the radioisotope is substantially inhibited by increasing either the internal or external unlabeled isotope concentration. The physical basis for the inhibition of radioisotope transport is mass action competition of the internal and external ^{40}Ca for the carrier. This type of inhibition is a general property of any transport cycle where the ligated ionophore states are in an approximate equilibrium determined by the divalent ion concentrations, and where the transport cycle is rate limited by a step(s) that occurs with each ion translocation. A more detailed analysis that involves ionophore ligation with protons and other ions would yield mass action competition of these ions with ^{45}Ca for the carrier. This type of effect has been described for protons and A23187 [27,28] and is an explanation for our observation of strontium inhibition of arachidonate-mediated ^{45}Ca efflux.

(B) Aqueous pores: mechanisms that are rate limited by activation steps that branch from the transport cycle

Efflux mechanisms of this type are exemplified by small aqueous pores and large aqueous pores. Single-channel studies have demonstrated that once activated, small aqueous pores such as calcium channels remain 'open' for several milliseconds and translocate ions with rates that are near the free diffusion limit: 10^6 to 10^8 s^{-1} [27,33,38,39]. With ion conductance this high, dissipation of the calcium gradient across the vesicle would occur in several milliseconds, i.e. during one 'opening' of the channel. Also, calcium movement via free diffusion through large aqueous pores is expected to occur very rapidly once the pore forms. As is the case with a small aqueous pore, the high free diffusion rate (i.e, $6 \cdot 10^{11}$ ions/s per pore for a 1.0 nm pore) ensures that a single defect would dissipate the calcium gradient across a vesicle in several microseconds. Because of the fast ion translocation rate with free diffusion and channel mechanisms, a rate-limiting 'activation' step would be required to give the type of average (integrated) calcium gradient dissipation that occurs over a period of many minutes in the platelet microsome system.

The model that is used to investigate the response of an activation limited mechanism (small or large aqueous pore) in a vesicular system to changes in internal and external calcium is based on the diagram in Fig. A-3. At an initial time ($t = 0$), n° vesicles have the same elevated internal concentration of calcium isotopes ($[^{45}Ca_i]^\circ$ and $[^{40}Ca_i]^\circ$). The activation of one channel or defect pore completely discharges the calcium gradient by repeatedly cycling through the translocation steps (for the case of a small aqueous pore) or via free diffusion (for the case of a large aqueous pore).

The internal $[^{45}Ca_i]$ concentration that is measured as a function of time (t) with a micropore filtration assay is an average value with a contribution ($\chi(t)$) from the vesicles that have not activated and contain the initial calcium concentration, and a contribution ($\eta(t)$) from vesicles that are effluxing the divalent cation.

$$\langle[^{45}Ca_i]\rangle = \chi(t) + \eta(t) \tag{A-5}$$

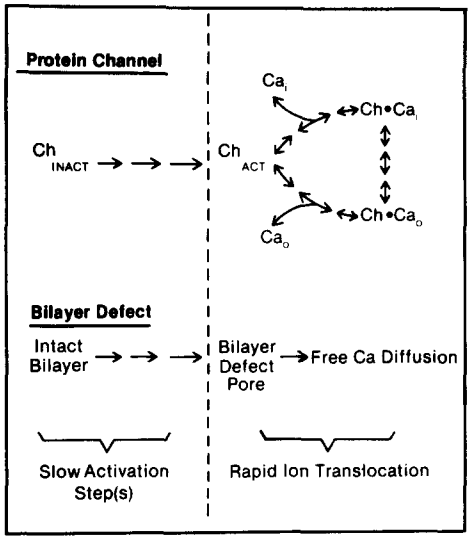

Fig. A-3. Aqueous pore protein channel and bilayer defect efflux mechanisms. Ch_{inact} and Ch_{act} refer to inactivated (closed) and activated (open) channel states, respectively. Ca_i, Ca_o, $Ch \cdot Ca_i$, and $Ch \cdot Ca_o$ refer to internal calcium, external calcium, ligated channel with calcium bound to inside facing pore binding site, and ligated channel with calcium bound to outside facing pore binding site, respectively.

An expression for $\chi(t)$ can be obtained by assuming that the formation of a defect or activation of a channel on a vesicle is described by a Poisson process [44] related to the following stochastic differential equation.

$$dP_n(t)/dt = k_a(n+1)P_{n+1}(t) - k_a n P_n(t) \tag{A-6}$$

where $P_n(t)$ and $P_{n+1}(t)$ are, respectively, the probability that the system contains n and $n+1$ vesicles that have not been 'activated'. Solution of this equation with the method of McQuarrie [44] gives the following expression for the expected number ($E\{n(t)\}$) of vesicles that have not formed a pore:

$$E\{n(t)\} = n^o e^{-k_a t} \tag{A-7}$$

Thus,

$$\chi(t) = [^{45}Ca_i]^o e^{-k_a t} \tag{A-8}$$

An expression for $\eta(t)$ can be obtained as diagrammed in Fig. A-4, and involves dividing the time domain before the measurement time (t) into j intervals of duration $\Delta\tau_j$, determining the residual calcium content at the measurement time (t) of the vesicles that became active during each interval $\Delta\tau_j$ (between time τ_0 and $\tau_j + \Delta\tau_j$), and then summing the results for all intervals $\Delta\tau_j$.

$$\eta(t) = \sum_{\text{all } \Delta\tau_j < t} (\text{number of vesicles activated in } \Delta\tau_j) \cdot (\text{calcium remaining after } t - \tau_j \text{ efflux period})$$

$$= \sum_j \Delta\chi_j(\tau_j + \Delta\tau_j)[^{45}Ca_i(t - \tau_j)] \tag{A-9}$$

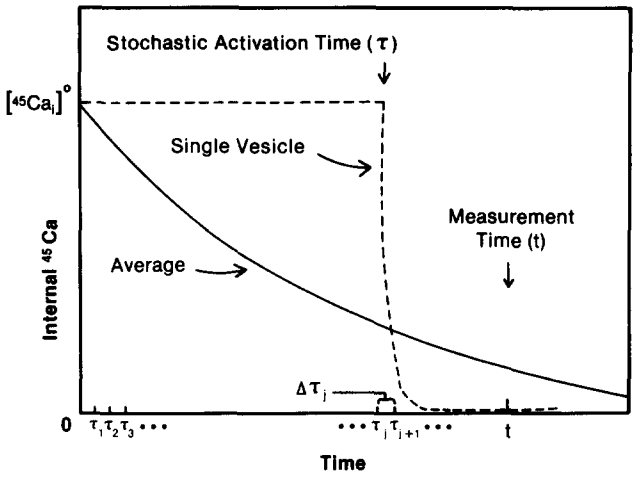

Fig. A-4. Stochastic calcium efflux out of vesicles through an aqueous pore. Measured average (———) and concentration in a single vesicle (– – –) that channel that activates (opens) at time j.

but

$$\Delta\chi_j = \frac{d\chi(\tau_j)}{d\tau}\Delta\tau$$

therefore,

$$\eta(t) = \sum_j [^{45}Ca_i(t - \tau_j)]\frac{d\chi_j}{d\tau}\Delta\tau_j$$

which can be expressed as a convolution integral upon performing the limit of $\Delta\tau_j \to 0$.

$$\eta(t) = \int_0^t [^{45}Ca_i(t - \tau)]\, d\chi(\tau)\, d\tau$$

$$= -k_a \int_0^t [^{45}Ca_i(t - \tau)]\, e^{-k_a t}\, d\tau \tag{A-10}$$

and thus the measured internal calcium can be expressed as

$$\langle[^{45}Ca(t)]\rangle = [^{45}Ca_i]^o e^{-k_a t} + -k_a \int_0^t [^{45}Ca(t - \tau)]\, e^{-k_a \tau}\, d\tau \tag{A-11}$$

Derivation of the exact algebraic form of the convolution integral (from the chemical rate equation for the case of a small aqueous pore or from the diffusion equation for a large aqueous pore) is not necessary because an upper limit to the magnitude of $\eta(t)$ can be easily established by considering the following inequality.

$$[^{45}Ca_i(t - \tau)] \le [^{45}Ca_i]^o e^{-k_c(t-\tau)} \tag{A-12}$$

where k_c is a characteristic constant with the value

$$k_c = |d([^{45}Ca(t - \tau)])/d\tau|_{max}/[^{45}Ca_i]^o \tag{A-13}$$

The upper limit to the magnitude of $\eta(t)$ is thus

$$\eta(t) \leq k_a[^{45}Ca_i]^o \int_0^t e^{-k_a\tau}\, e^{-k_c(t-\tau)}\, d\tau$$

$$\leq [^{45}Ca_i]^o \frac{k_a}{k_a - k_c}(e^{-k_a t} - e^{-k_c t}) \quad \text{(A-14)}$$

(i) Small aqueous pores (i.e., calcium channel)

Studies with single channels [27,33,38,39] indicate that the rate-limiting step for ion translocation by a selective small aqueous pore at ion concentrations above the channel ligation K_d value involves the disassociation of the ion from the external ligation site, and not the rapid diffusion limited ion translocation step. With a rate-limited disassociation step the following expression is obtained.

$$-d([^{45}Ca_i(t)])/dt = k[Ch \cdot {}^{45}Ca_o] \quad \text{(A-15)}$$

With an equilibrium assumption involving internal channel ligation and symmetric ion translocation, the following steady-state rate formula is obtained.

$$-d([^{45}Ca_i(t)])/dt = (k[Ch_{act}][^{45}Ca_i])(K_d + [^{45}Ca_i]^o + [^{40}Ca_i]^o + [^{45}Ca_o]^o + [^{40}Ca_o]^o)^{-1} \quad \text{(A-16)}$$

where $[Ch_{act}]$ is the total concentration of activated channel, k is the rate constant for ion disassociation, and K_d is the disassociation constant for channel ligation. Thus:

$$k_c = \frac{k[Ch_{act}]}{K_d + 2[^{40}Ca_i]^o + 2[^{45}Ca_i]^o} \quad \text{(A-17)}$$

For a 300 nm vesicle with one channel ($[Ch_{act}] = 1.17 \cdot 10^{-7}$ M with respect to internal volume of $1.41 \cdot 10^{-17}$ l) that has K_d, k, and k_a values of 10^{-4} M, 10^5 s^{-1} and 10^{-3} s^{-1}, and with divalent ion concentrations of 10 mM, 0.1 mM, 0.01 mM and 0.0001 mM for $[^{40}Ca_i]^0$, $[^{45}Ca_i]^0$, $[^{40}Ca_o]^o$, and $[^{45}Ca_o]^o$, the value of k_c from Eqn. A-17 is approx. 0.6 s^{-1}. The percentage maximum contribution of $\eta(t)$ with this k_c value to the measured average calcium concentration (Eqn. A-5) is 0.167%, approximately two orders of magnitude below the precision limit of the micropore filtration assay. The value of k_c could thus be changed by four to five log units through manipulation of internal or external calcium concentrations without a measurable effect on $\langle[^{45}Ca_i(t)]\rangle$. Also, similar large changes in the rate constant of the translocation step and/or channel affinity for calcium would be unmeasurable. This mathematical development demonstrates that the vast majority of the vesicles contain the initial concentration of internal calcium or have a completely discharged calcium gradient; only a small fraction are actively effluxing and are thus sensitive to variations in divalent cation concentration. Thus, while sensitivity of a channel to calcium concentration can be demonstrated in planer bilayers or in a vesicle system where efflux occurs in milliseconds, vesicular efflux that is rate limited by channel opening and occurs over a period of minutes would be insensitive to calcium concentrations.

(ii) Large aqueous pore (i.e., detergent defect)

For the case of free diffusion through a large aqueous pore, the gradient dissipation occurs in accordance to Frick's free diffusion relationship.

$$d([^{45}Ca_i(t)])/dt = -DA[^{45}Ca_i(t)]/MV \quad \text{(A-18)}$$

where D, A, M, and V are the diffusion constant, the pore area, the channel length, and the volume of the vesicle. The characteristic constant from Eqn. A-13 is thus

$$k_c = DA/MV \quad \text{(A-19)}$$

For a 5.0 nm pore across a 5 nm thick membrane on a vesicle with a volume of $1.41 \cdot 10^{-17}$ liters (300 nm diameter) and a D value of $1 \cdot 10^{-5}$ cm/s [41], k_c assumes a value of approx. 350 s^{-1}. With a k_a value of 10^{-3} s, the percentage contribution of the $\eta(t)$ term to the value of $\langle[^{45}Ca_i(t)]\rangle$ would be $2.91 \cdot 10^{-4}$%. The small contribution of the $\eta(t)$ term to the average calcium measurement, when considered with the observation that the calcium diffusion coefficient is a weak function of calcium concentration [41], demonstrates that a free diffusion mechanism would be insensitive to variation in intra- and extravesicular calcium.

Acknowledgements

This research was supported by a Specialized Center of Research in Thrombosis (HL26309) and an American Heart Association Grant-in-Aid Award (87-0803). Dr. Griffin was supported by an NIH Training Grant (HL07149). The authors wish to thank Dr. G.C. LeBreton for providing 13-azaprostanoic acid for these studies.

References

1 Rink, T., Smith, S. and Tsien, R. (1982) FEBS Lett. 148, 21–27.
2 Rao, G.H.R., Peller, D. and White, J.G. (1985) Biochem. Biophys. Res. Commun. 132, 652–657.
3 Pollock, W.K., Rink, T.J. and Irvine, R.F. (1986) Biochem. J. 235, 869–877.
4 Ware, J.A., Johnson, P.C., Smith, M. and Salzman, E.W. (1986) J. Clin. Invest. 77, 878–886.
5 Gerrard, J., Butler, A., Graff, G., Stoddard, S. and White, J.G. (1978) Prostaglandins and Medicine 1, 373–385.

6 Gerrard, J. and White, J.G. (1978) Prog. Hemostas. Thrombos. 4, 87–125.
7 Gerrard, J., Butler, A., Peterson, D.A., Stoddard, S. and White, J.G. (1978) Prostaglandins and Medicine 1, 387–396.
8 White, II, G.C. and Raynor, S.T. (1982) Biochem. Biophys. Res. Commun. 104, 1066–1072.
9 Berridge, M.J. (1984) Biochem. J. 220, 345–360.
10 Brass, L.F. and Joseph, S.K. (1985) J. Biol. Chem. 260, 15172–15179.
11 O'Rourke, F., Halenda, S.P., Zavoico, G.B. and Feisntein, M.B. (1985) J. Biol. Chem. 260, 956–962.
12 Authi, K. and Crawford, N. (1985) Biochem. J. 230, 247–253.
13 Adunyah, S. and Dean, W.L. (1985) Biochem. Biophys. Res. Commun. 128, 1274–1280.
14 O'Rourke, F., Zavoico, G.B., Smith, Jr., L.H. and Feinstein, M.B. (1987) FEBS Lett. 214, 176–180.
15 Banga, H.S., Simons, E.R., Brass, L.F. and Rittenhouse, S.E. (1986) Proc. Natl. Acad. Sci. USA 83, 9197–9203.
16 Fisher, G., Bakshian, S. and Baldassare, J. (1985) Biochem. Biophys. Res. Commun. 129, 958–964.
17 Hamberg, M. (1976) Biochim. Biophys. Acta 431, 651–654.
18 Daniel, J.L., Dangelmaier, C.A., Selak, M. and Smith, J.B. (1986) FEBS Lett. 206, 299–302.
19 Fischer, T.H., Campbell, K.P. and White, II, G.C. (1985) J. Biol. Chem. 260, 8996–9001.
20 Peterson, G. (1977) Anal. Biochem. 83, 346–356.
21 Bartlett, G. (1959) J. Biol. Chem. 234, 466–468.
22 Fabiato, A. and Fabiato, F. (1979) J. Physiol. (Paris) 75, 463–505.
23 Allen, T., Romans, A., Kercret, H. and Segrest, J. (1980) Biochim. Biophys. Acta 601, 328–342.
24 Fischer, T.H. and Lasic, D. (1984) Mol. Cryst. Liq. Cryst. 102, 141–145.
25 Le Peuch, C.J., Le Peuch, D.A.M., Datz, S., Demaille, J.G., Hincke, M.T., Bredoux, R., Enouf, J., Lévy-Tolédano, S. and Caen, J.P. (1983) Biochim. Biophys. Acta 731, 456–464.
26 Meyer, T., Holowka, D. and Stryer, L. (1988) Science 240, 653–656.
27 Pfeiffer, D., Taylor, R. and Lardy, H. (1978) Ann. N.Y. Acad. Sci. 307, 402–423.
28 Kolber, M. and Haynes, D. (1981) Biophys. J. 36, 369–391.
29 Tanford, C. (1980) in The Hydrophobic Effect, p. 90, Wiley-Interscience Press, New York, NY.
30 Rybicki, J., Venton, D. and Le Breton, G.C. (1983) Biochim. Biophys. Acta 751, 66–73.
31 Kellogg, E. and Firdovich, I. (1975) J. Biol. Chem. 250, 8812–8817.
32 Serhan, C., Anderson, P., Goodman, E., Dunham, P. and Weissmann, G. (1981) J. Biol. Chem. 256, 2736–2741.
33 Moczydlowski, E. (1986) in Ion Channel Reconstitution (Miller, C., ed.), p. 75, Plenum Press, New York, NY.
34 Garcia, A. (1986) in Ionic Channels in Cells and Model Systems (Latorre, R., ed.), p. 127, Plenum Press, New York, NY.
35 Bernhardt, J. and Neumann, E. (1980) J. Theor. Biol. 86, 649–650.
36 Heidmann, T., Bernhardt, J., Neumann, E. and Changeux, J. (1983) Biochemistry 22, 5452–5459.
37 Meissner, G., Darling, E. and Eveleth, J. (1986) Biochem. 25, 236–244.
38 Eisenberg, M., Hall, J. and Mead, C. (1973) J. Membr. Biol. 14, 143–176.
39 McCleskey, E., Fox, A., Feldman, D. and Tsien, R. (1986) J. Exp. Biol. 124, 177–190.
40 Polymeropoulos, E. and Brinckmann, J. (1985) Annu. Rev. Biophys. Biophys. Chem. 14, 315–330.
41 Weast, R. (1985) in CRC Handbook of Chemistry and Physics, 65th Edn. (Weast, R., Astle, M. and Beyer, W., eds.), p. F-45, CRC Press, Inc., Boca Raton, FL.
42 Läuger, P. (1980) J. Membr. Biol. 57, 163–178.
43 Fischer, T.H., Campbell, K.P. and White, II, G.C. (1987) Biochemistry 26, 8024–2030.
44 McQuarrie, D. (1962) J. Chem. Physics 38, 433–437.